Available online at www.sciencedirect.com
SCIENCE DIRECT
Catalysis Today 100 (2005) 133–144
CATALYSIS TODAY
www.elsevier.com/locate/cattod

Electrochemical promotion of catalysis: mechanistic investigations and monolithic electropromoted reactors

D. Tsiplakides, S. Balomenou, A. Katsaounis, D. Archonta, C. Koutsodontis, C.G. Vayenas *

Department of Chemical Engineering, Caratheodory 1 St., University of Patras, GR-26504 Patras, Greece

Available online 7 March 2005

Abstract

Recent progress is surveyed both in elucidating the mechanism of electrochemical promotion at the molecular level and in utilizing it in monolithic electropromoted catalytic reactors. On the mechanistic side, recent $^{18}O_2$ TPD and $^{18}O_2$ + CO TP reaction studies have confirmed, together with STM, the validity of the sacrificial promoter model for both electrochemical promotion and metal–support interactions of Pt and Rh with anionic (YSZ) and mixed anionic-electronic supports. On the practical side, two recent advances are discussed, i.e., the electropromotion of thin (40 nm) sputtered catalyst films, with metal dispersion of the order of 20%, and the development of the monolithic electropromoted reactor (MEPR) which is a hybrid between a monolithic catalytic reactor and a flat-plate solid oxide fuel cell and allows for compact design and easy scale-up and scale-down of electropromoted catalytic units.

Keywords: Electrochemical promotion; NEMCA effect; Spillover-backspillover phenomena; Metal–support interactions; Monolithic electropromoted reactor (MEPR); Ethylene oxidation on Pt and Rh; NO reduction on Rh; STM observation of spillover-backspillover; $^{18}O_2$ TPD on Pt/YSZ; $^{18}O_2$ + CO TP reaction on Pt/YSZ

1. Introduction

Electrochemical promotion of catalysis [1–15] and metal–support interactions with ionically conducting (Y_2O_3-stabilized-ZrO_2, YSZ) or mixed ionic-electronic conductors (ZrO_2, CeO_2, TiO_2, W^{6+}-doped-TiO_2) [15–25] are phenomena which both affect the chemisorptive and catalytic properties of metal catalysts in a very pronounced manner. The term electrochemical promotion [1–15] is used to describe the very pronounced changes observed in the catalytic properties of conductive catalysts deposited on solid electrolytes upon application of electrical currents or potentials (typically up to ±2 V) between the catalyst and a second electronic conductor (counter electrode) also deposited on the solid electrolyte support, while metal–support interactions of nanodispersed catalysts are the cause for the change in catalytic activity or selectivity of the active phase observed upon varying the catalyst support [15–25].

In the case of electrochemical promotion of catalysis (EPOC or NEMCA effect or electropromotion) the metal catalyst is usually in the form of a porous and electronically conducting film deposited on the solid electrolyte (e.g. O^{2-} or mixed O^{2-}-electronic conductor) while in the case of metal–support interactions (MSI) the metal is in the form of nanoparticles deposited on the porous O^{2-} or mixed O^{2-}-electronic conducting support.

It has been recently shown via several techniques [14,15,26–29] including STM [27] that the two phenomena are closely related and mechanistically equivalent as they both stem from the migration (reverse spillover) of anionic $O^{\delta-}$ species from the support to the metal-gas interface. These backspillover $O^{\delta-}$ species together with their image charge in the metal create an overall neutral double layer at the metal-gas interface and thus affect both chemisorption and catalysis at this interface in a pronounced manner. At high oxygen coverages the backspillover $O^{\delta-}$ species are distinct from, and more strongly adsorbed than, oxygen adsorbed from the gas phase. They are also less reactive for catalytic oxidations than gas-supplied oxygen and thus act as sacrificial promoters [14,15]. The backspillover is thermal in

* Corresponding author. Fax: +30 2610 997269.
E-mail address: cat@chemeng.upatras.gr (C.G. Vayenas).

0920-5861/$ – see front matter © 2004 Elsevier B.V. All rights reserved.
doi:10.1016/j.cattod.2004.12.015

the case of metal support interactions (MSI) and electrochemically assisted in the case of NEMCA [14,15,26,30], as shown in the latter case by numerous surface spectroscopic (XPS, UPS, TPD, STM) and electrochemical (AC Impedance, cyclic voltammetry) techniques [15,26–30].

The first thorough review of electrochemical promotion was given in Catalysis Today several years ago [31]. Several reviews followed [13,32–37] including a recent book [14] which discusses in detail the close relationship between electrochemical promotion and metal–support interactions. The basic phenomenology of EPOC when using O^{2-} or H^+ conducting supports is given in Figs. 1 and 2 respectively. In the former case (Fig. 1, [14]) the (usually porous) metal (Pt) catalyst-electrode, typically 40 nm to 4 μm thick, is deposited on an 8 mol% Y_2O_3-stabilized-ZrO_2 (YSZ) solid electrolyte.

In the latter case (Fig. 2, [6]) the nanodispersed Pd catalyst is deposited on porous conductive graphitic C which is supported on Nafion, a H^+ conductor.

In both cases under open-circuit operation ($I = 0$, no electrochemical rate) there is a catalytic rate, r_0, of ethylene consumption for oxidation to CO_2 (Fig. 1) or of 1-butene consumption due to reduction to butane and isomerization to *cis*-2-butene and *trans*-2-butene (Fig. 2).

Application of an electrical current, I, or potential (U_{WR}) between the catalyst and a counterelectrode and thus changing the catalyst potential, U_{WR}, with respect to a reference electrode, causes very pronounced and strongly non-Faradaic (i.e. $\Delta r \gg I/2F$ in Fig. 1, $\Delta r \gg |-I/F|$ in Fig. 2) alterations to the catalytic rate (Figs. 1 and 2) and to the product selectivity (Fig. 2).

Two parameters are commonly used to describe the magnitude of electrochemical promotion:

1. The apparent Faradaic efficiency, Λ, defined from:

$$\Lambda = \frac{\Delta r_{\text{catalytic}}}{(I/2F)} \tag{1}$$

where $\Delta r_{\text{catalytic}}$ is the current- or potential-induced change in catalytic rate, I is the applied current and F is Faraday's constant.

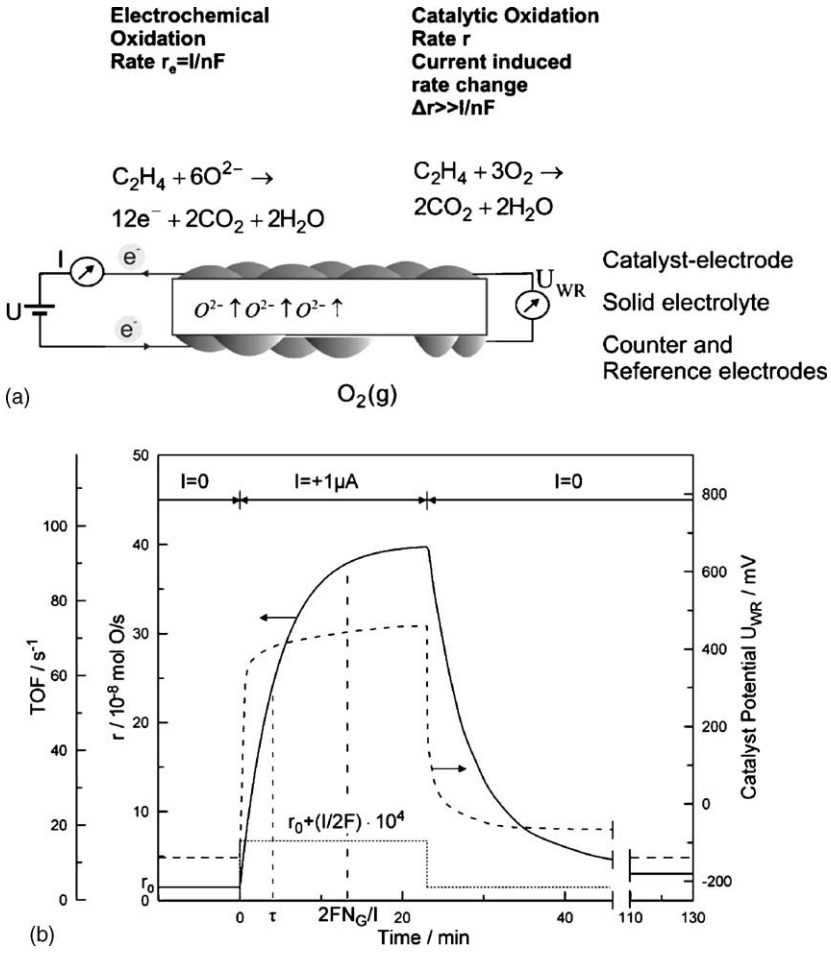

Fig. 1. (a) Basic experimental setup and operating principle of electrochemical promotion with O^{2-} conducting supports. (b) Catalytic rate, r, and turnover frequency, TOF, response of C_2H_4 oxidation on Pt deposited on YSZ, an O^{2-} conductor, upon step changes in applied current. $T = 370\ ^\circ C$, $p_{O_2} = 4.6$ kPa, $p_{C_2H_4} = 0.36$ kPa. Also shown (dashed line) is the catalyst-electrode potential, U_{WR}, response with respect to the reference, R, electrode. The catalytic rate increase, Δr, is 25 time larger than the rate, r_0, before current application and 74,000 times larger than the rate, $I/2F$, of O^{2-} supply to the catalyst-electrode. N_G is the Pt/gas interface surface area, in mol Pt and TOF is the catalytic turnover frequency (mol O reacting per surface Pt mol/s). Reprinted with permission from Kluwer/Plenum Publishers [14].

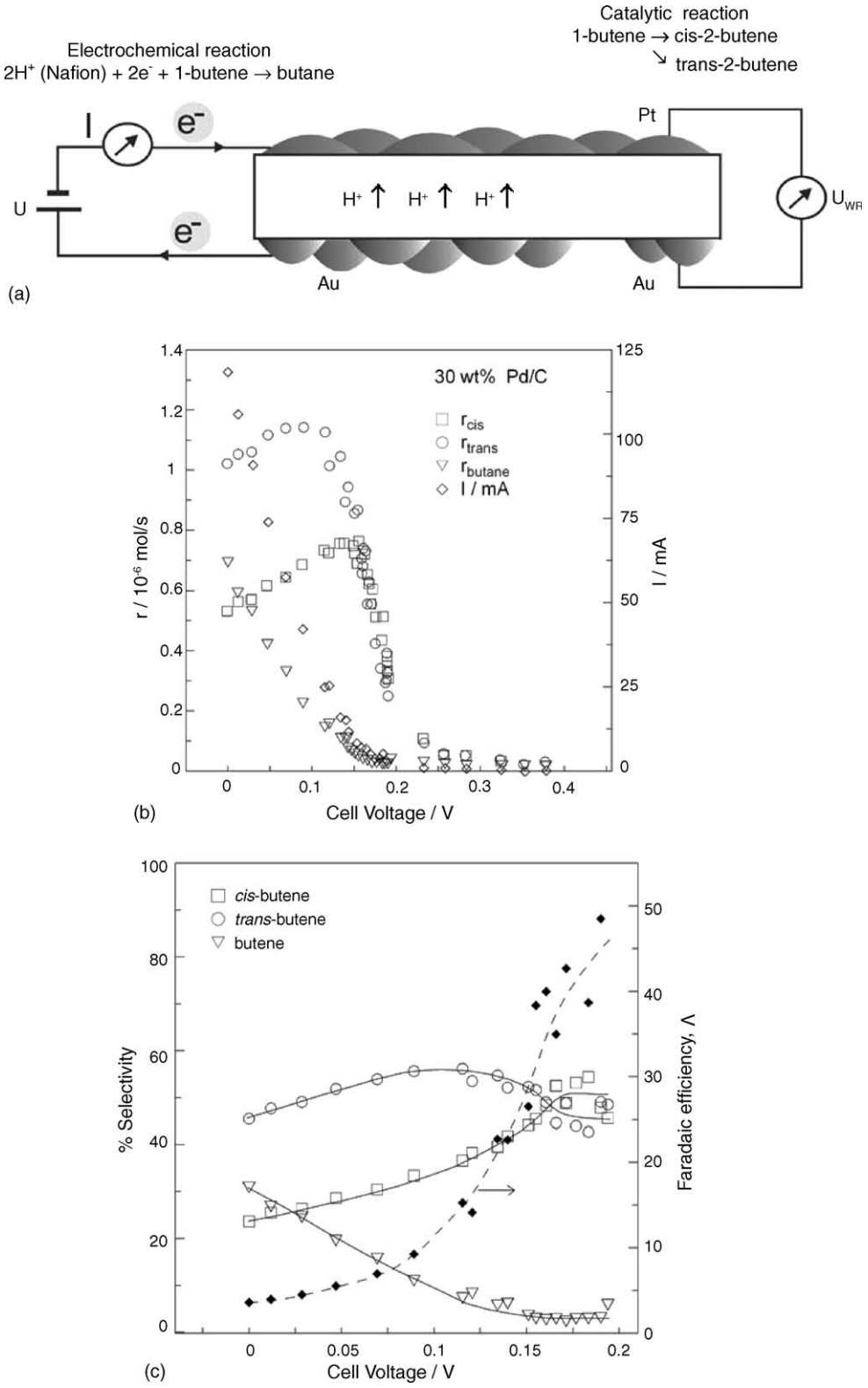

Fig. 2. (a) Basic experimental setup and operating principle of electrochemical promotion using a H^+ conductor during 1-butene isomerization to *cis*-2-butene and *trans*-2-butene on C supported Pd [6]. (b) Electrochemical promotion of the isomerization reaction [6]. Steady-state effect of cell potential on the cell current, I, and on the rates of formation of *cis*-2-butene, *trans*-2-butene and butane produced from 1-butene supplied over a dispersed Pd/C catalyst-electrode deposited on Nafion, a H^+ conductor [6]. (c) Corresponding effect of cell potential on the selectivities to *cis*-2-butene, *trans*-2-butene and butane and on the apparent Faradaic efficiency, Λ, defined as $\Delta r_{\text{total}}/(I/F)$. Thus, each proton catalyzes the isomerization of up to 50 molecules of 1-butene to *cis*- and *trans*-2-butene [6].

2. The rate enhancement, ρ, defined from:

$$\rho = \frac{r}{r_0} \tag{2}$$

where r is the electropromoted catalytic rate and r_0 is the unpromoted (open-circuit) catalytic rate.

A reaction exhibits electrochemical promotion when $|\Lambda| > 1$, while electrocatalysis is limited to $|\Lambda| \leq 1$. A reaction is termed electrophobic when $\Lambda > 1$ and electrophilic when $\Lambda < -1$. In the former case the rate increases with catalyst potential, U, while in the latter case the rate decreases with catalyst potential. Λ values up to 3×10^5 [1,13,14] and ρ values up to 150 [14] have been found for several systems. More recently ρ values between 300 [38] and 1200 [39,40] have been measured for C_2H_4 oxidation on Pt.

In the experiment of Fig. 1, it is $\Lambda = 74{,}000$ and $\rho = 26$, i.e., the rate of C_2H_4 oxidation increases by a factor of 25 and the increase in the rate of O consumption is 74,000 times larger than the rate, $I/2F$, of O^{2-} supply to the catalyst. In the experiment of Fig. 2 the maximum ρ values for the production of *cis*-2-butene, *trans*-2-butene and butene are of the order of 50 and the corresponding maximum Λ values are of the order of 40 for *cis*-2-butene formation, 10 for *trans*-2-butene formation and less than one for butene formation. Thus, each proton supplied to the Pd catalyst can cause the isomerization of up to 40 1-butene molecules to *cis*-2-butene and up to 10 1-butene molecules to *trans*-2-butene while the hydrogenation of 1-butene to butane is electrocatalytic, i.e., Faradaic.

Up to 2001 [14], more than 70 different catalytic reactions (oxidations, hydrogenations, dehydrogenations, isomerizations, decompositions) have been electrochemically promoted on Pt, Pd, Rh, Ag, Au, Ni, IrO_2, RuO_2 catalysts deposited on O^{2-} (YSZ), Na^+ (β''-Al_2O_3), H^+ ($CaZr_{0.9}In_{0.1}O_{3-\alpha}$, Nafion [6,41]), F^- (CaF_2), aqueous [42,43], molten salt [44] and mixed ionic-electronic (TiO_2 [45], CeO_2 [46]) conductors.

Clearly EPOC is not limited to any particular class of conductive catalyst, catalytic reaction or ionic support. Some real-scale electrochemically promoted soot combustion units have been recently produced by Dinex in Denmark [14].

Although electrochemical promotion has been studied for over seventy catalytic systems [14], there has been so far no large scale commercial utilization of electrochemical promotion. There were two main reasons for this:

(a) Expensive thick catalyst films (typically 0.1–5 μm thick) with metal dispersion below 0.01%.
(b) Lack of efficient and compact reactor designs allowing for the utilization of electrochemical promotion with a minimum of electrical connections to the external power supply.

As shown recently [47] both of these limitations can be overcome via the use of thin sputtered noble metal electrodes with metal dispersion exceeding 15% in novel electrochemically promoted reactors (MEPR) of the type briefly surveyed here.

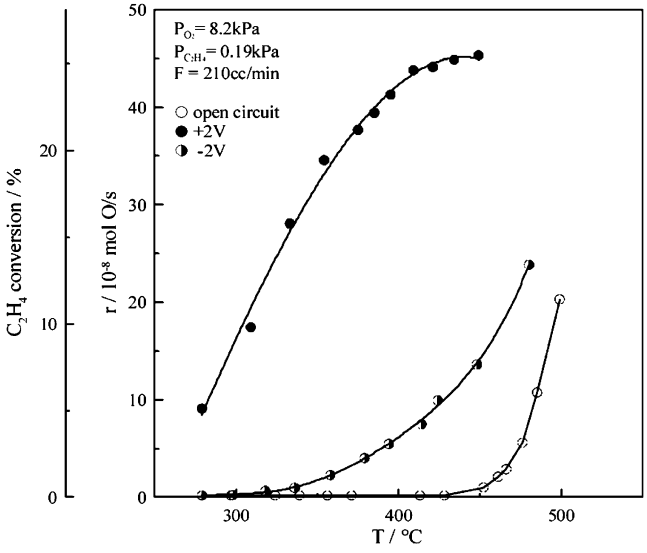

Fig. 3. Effect of temperature on the rate of C_2H_4 oxidation on Pt deposited on YSZ under open-circuit and under anodic (+2 V) and cathodic (−2 V) polarization [38].

2. Magnitude of electrochemical promotion and the sacrificial promoter mechanism

The magnitude of electrochemical promotion can be assessed from Fig. 3 which shows the temperature dependence of the rate of C_2H_4 oxidation on a Pt film deposited on YSZ under open-circuit conditions and under anodic (+2 V) and cathodic (−2 V) polarization. The Pt catalyst-working electrode was prepared by application of a thin coating of Pt paste on one side of an yttria-stabilized zirconia (YSZ 8 mol%) pellet followed by calcination in air for 1.5 h at 430 °C and then for 30 min at 830 °C, leading to a porous 0.24 μm thick Pt film. Gold counter and reference electrodes were also deposited on the reverse side of the pellet using the same method [14]. The experiments were carried out in a single-chamber reactor [14]. Anodic polarization causes a 200 °C decrease in the catalyst light-off temperature and leads to rate enhancement ρ values of the order of 300 [38] with Faradaic efficiency, Λ, values of the order of 500 [38]. Negative polarization also significantly enhances the catalytic rate, as it enhances the chemisorption of ethylene on the catalyst surface [14,38]. Ethylene oxidation on Pt exhibits at high temperatures ''inverted volcano'' behaviour, i.e., the rate is enhanced both with increasing and decreasing catalyst potential.

It has been shown recently [14,30] that the catalytic rate dependence on catalyst potential or work function [1,14] can be predicted on the basis of the rate dependence on the partial pressures of the electron donor and electron acceptor

reactant [14,30]. These rigorous electrochemical and classical promotional rules appear to have no exceptions in the published electropromotion [14,30] and classical promotion literature [48].

The molecular origin of electrochemical promotion has been for years rationalized on the basis of the sacrificial promoter mechanism [14]. According to this mechanism, NEMCA results from the Faradaic (i.e. at a rate I/nF) introduction of promoting species ($O^{\delta-}$ in the case of O^{2-} conductors, H^+ in the case of H^+ conductors) on the catalyst surface. This electrochemically introduced O^{2-} species acts as a promoter for the catalytic reaction (by changing the catalyst work function and affecting the chemisorptive bond strengths of coadsorbed reactants and intermediates) and is eventually consumed at a rate equal, at steady state, to its rate of supply ($I/2F$) which is Λ times smaller than the rate of consumption of the catalytic reactant, e.g. atomic O originating from the gas phase [14].

Fig. 4 shows the validity of the sacrificial promoter concept for the galvanostatic transient of Fig. 1, by presenting O_2 TPD (Fig. 4b) and cyclic voltammetric (Fig. 4c) spectra obtained at times corresponding to those of the NEMCA galvanostatic transient of C_2H_4 oxidation (Fig. 4a, [14]), under high vacuum conditions. The sample consists of a polycrystalline Pt catalyst film deposited in the form of a half-ring on the outer surface of a tubular YSZ specimen with Au counter and reference electrodes deposited on the inside wall of the tubular YSZ element opposite to the Pt-film. The sample is first exposed to gaseous oxygen followed by electrochemically supplied oxygen from the solid electrolyte. A linear temperature increase (Fig. 4b) or cyclic potential variation (Fig. 4c) is used to obtain the corresponding TPD spectra or cyclic voltammograms. One clearly observes, both with TPD and with cyclic voltammetry, the Faradaic introduction, over a time period $2FN_G/I$, (where N_G is the catalyst surface area expressed in mol and thus $2FN_G/I$ is the time required to form a monolayer of O^{2-} on the catalyst surface) of a second (backspillover) strongly bonded oxygen species on the Pt catalyst surface which displaces the normally chemisorbed oxygen state to lower desorption temperatures. This displacement, which results from strong repulsive lateral interactions, between O^{2-} and more covalently bonded atomic oxygen [14], causes the observed dramatic enhancement in the catalytic rate. The backspillover O^{2-} state acts as a sacrificial promoter.

This molecular picture has been recently confirmed by the use of $^{18}O_2$ TPD [49] (Fig. 5) which confirms that for the electropromoted Pt/YSZ catalyst the displaced weakly bonded state (β_2) is populated by gaseous oxygen (^{18}O) while the strongly bonded-promoting state β_3 is populated by backspillover lattice oxygen ^{16}O. This fully confirms the sacrificial promoter mechanism of electrochemical promotion [14,49].

As also shown in Fig. 5, there is a strong and noteworthy similarity in the O_2 TPD spectra of electro-

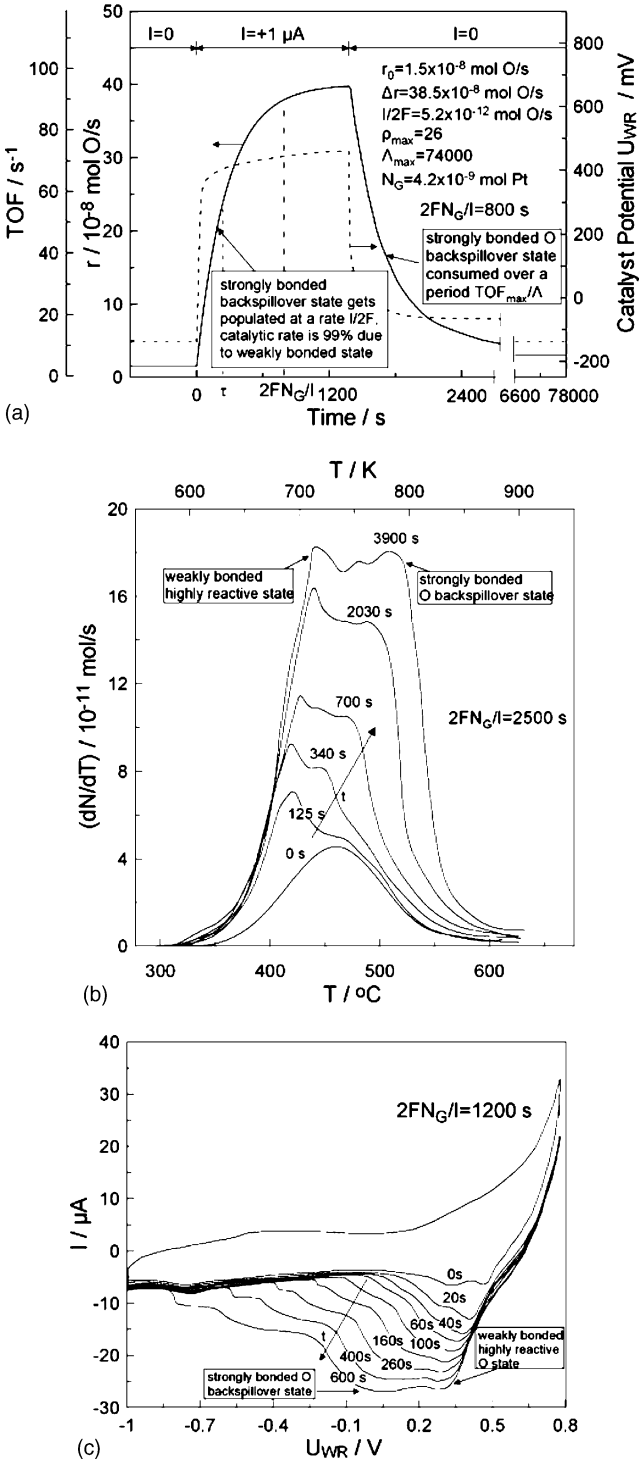

Fig. 4. NEMCA and its origin on Pt/YSZ catalyst electrodes [14]. Transient effect of the application of a constant current (a and b) or constant potential U_{WR} (c) on (a) the rate, r, of C_2H_4 oxidation on Pt/YSZ (also showing the corresponding U_{WR} transient) (b) the O_2 TPD spectrum on Pt/YSZ after current ($I = 15$ μA) application for various times t. (c) The cyclic voltammogram of Pt/YSZ after holding the potential at $U_{WR} = 0.8$ V for various times t [14].

promoted Pt films deposited on YSZ and Pt/YSZ powder catalysts. The only difference is that, in the case of the Pt/YSZ powder, lattice oxygen also occupies state β_2

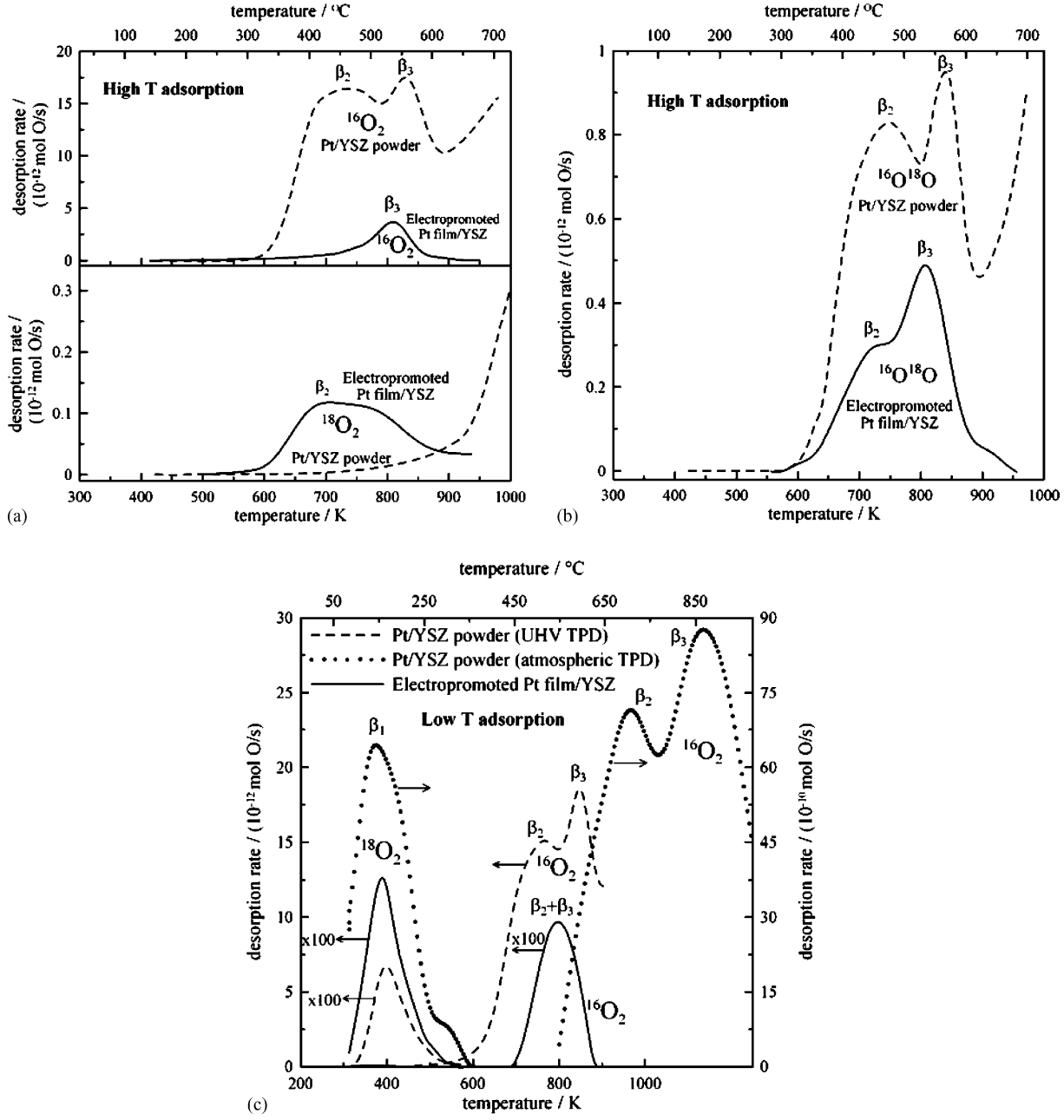

Fig. 5. Comparison of oxygen thermal desorption spectra from nanodispersed Pt/YSZ catalyst (1%Pt/YSZ) and from Pt/YSZ film taken under UHV conditions [49]. (a) Comparison of desorption of $^{18}O_2$ and $^{16}O_2$, high T_{ad} (200 °C) adsorption; (b) comparison of $^{16}O^{18}O$ desorption, high T_{ad} (200 °C) adsorption; desorption was performed with linear heating rate, $\beta = 0.5$ °C/s; (c) comparison of O_2 TPD spectra of the nanodispersed Pt/YSZ catalyst (UHV TPD and atmospheric pressure TPD) and of the electrochemically promoted Pt/YSZ film for low adsorption temperature, $T_{ad} = 70$ °C. Heating rate $\beta = 0.5$ °C/s for the film and the UHV powder TPD and 1.5 °C/s up to 750 °C followed by 0.35 °C above 750 °C for the atmospheric pressure power TPD [49].

(Fig. 5a) and gaseous oxygen $^{18}O_2$ is limited to the low temperature desorption peak β_1 [49]. The latter appears both with the dispersed Pt/YSZ powder catalysts and with the electropromoted Pt film/YSZ catalysts. These results corroborate the functional identity and only operational difference between electrochemical promotion and metal–support interactions with O^{2-} conducting supports [14,26].

The O^{2-} backspillover mechanism of electrochemical promotion and metal–support interaction has been also confirmed recently via STM [27], as shown in Fig. 6. Anodic polarization causes the decoration of the Pt(1 1 1) surface of a Pt single crystal which is interfaced with the YSZ support, with backspillover O^{2-} species which form a Pt(1 1 1)–(12 × 12)–O adlattice which coexists with the well known underlying Pt(1 1 1)–(2 × 2)–O adlattice formed by gaseous O_2 [27].

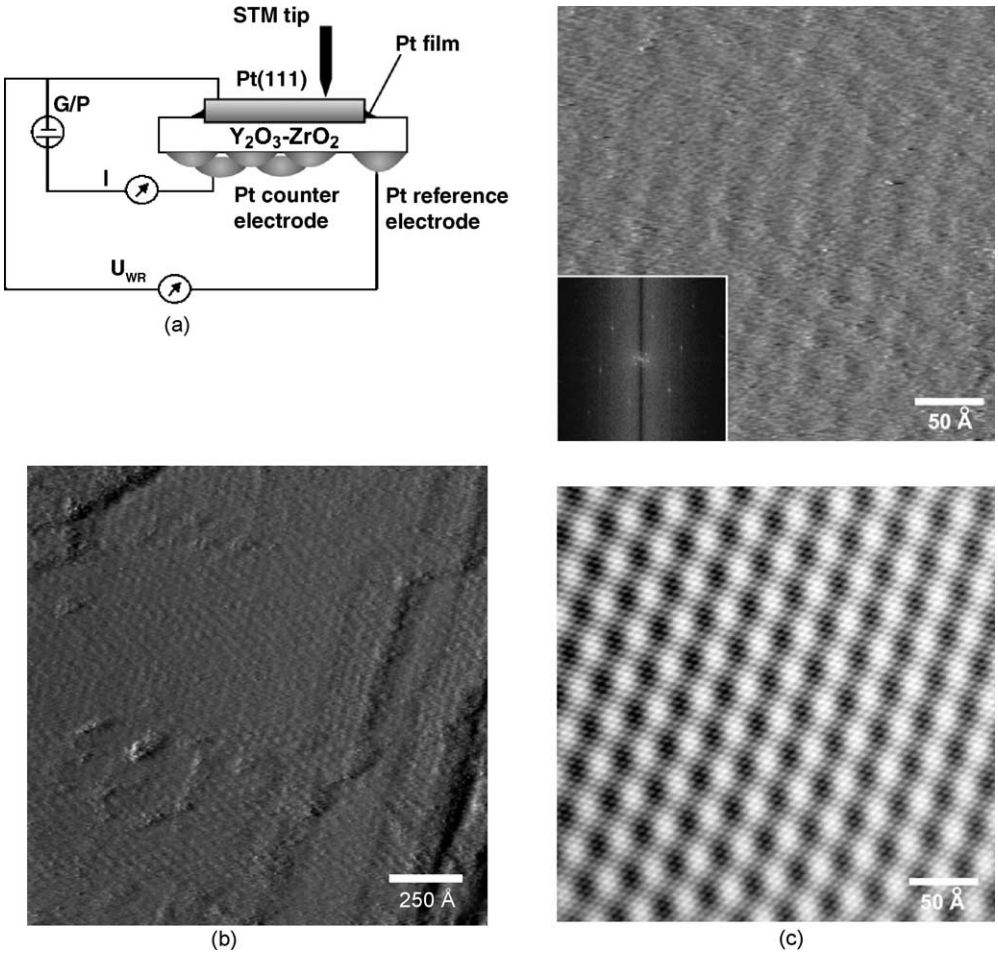

Fig. 6. (a) Schematic of the experimental setup used to investigate via STM the Pt(1 1 1) catalyst-electrode surface. G/P is the galvanostat-potentiostat and U_{WR} is the catalyst potential with respect to the reference electrode. (b) Unfiltered STM image of a 1275 Å × 1275 Å area of the Pt(1 1 1) surface following positive potential application (U_{WR} = 1 V) (bias U_t = 450 mV, tunneling current I_t = 7 nA). (c) Unfiltered (top) and filtered (bottom) STM image of the Pt(1 1 1) surface following positive potential application (U_{WR} = 1 V) showing the backspillover O^{2-}-formed Pt(1 1 1)–(12 × 12)–O adlattice overlapping with the underlying Pt(1 1 1)–(2 × 2)–O adlattice. Inset shows the Fourier transform spectrum (bias U_t = 400 mV, tunneling current I_t = 8 nA) [27].

3. Electropromotion of thin sputtered catalyst films in novel monolithic reactors

Several very recent studies [47,50] have confirmed the feasibility of electrochemically promoting thin (typically 40 nm) sputtered metal films with metal dispersion higher than 10–20% [47]. This is an important practical breakthrough, because in these films the metal dispersion and utilization is comparable to that of state-of-the art conventional supported catalysts. Some new results are presented below in conjunction with the novel flat-plate electropromoted reactors.

The recently developed novel monolithic electropromoted reactor (MEPR) [47], consists of flat (Fig. 7) or ribbed [47] solid electrolyte plates, covered on both sides by appropriate thin porous conductive catalyst layers. The plates are inserted in appropriately carved grooves on the inside surfaces of the walls of the ceramic reactor casing. These surfaces are also used to create two current collectors, one establishing electrical contact among all catalyst films deposited on the top side of the plates (catalyst 1), the other current collector establishing electrical contact with all catalyst films deposited on the bottom side of the plates (catalyst 2, which can also be an inert conductive material). In this way, all catalyst films can be electrochemically promoted (anodically for catalyst 1 or 2, cathodically for catalyst 2 or 1) via only two external connecting wires (Fig. 7). This is a significant practical simplification and the MEP reactor can be considered as a hybrid between a classical monolithic honeycomb reactor (of which it has all the geometric dimensions) and of a flat- or ribbed-plate solid oxide fuel cell [51]. Contrary to the case of fuel cells, where the fuel and air gas streams are kept separated, in the case of the MEP reactor there is only one gas stream containing all reactants and products, as in every classical catalytic reactor.

An additional advantage of the MEP reactor is that it can be assembled and dismantled at will and its flat or ribbed plates can be replaced whenever necessary.

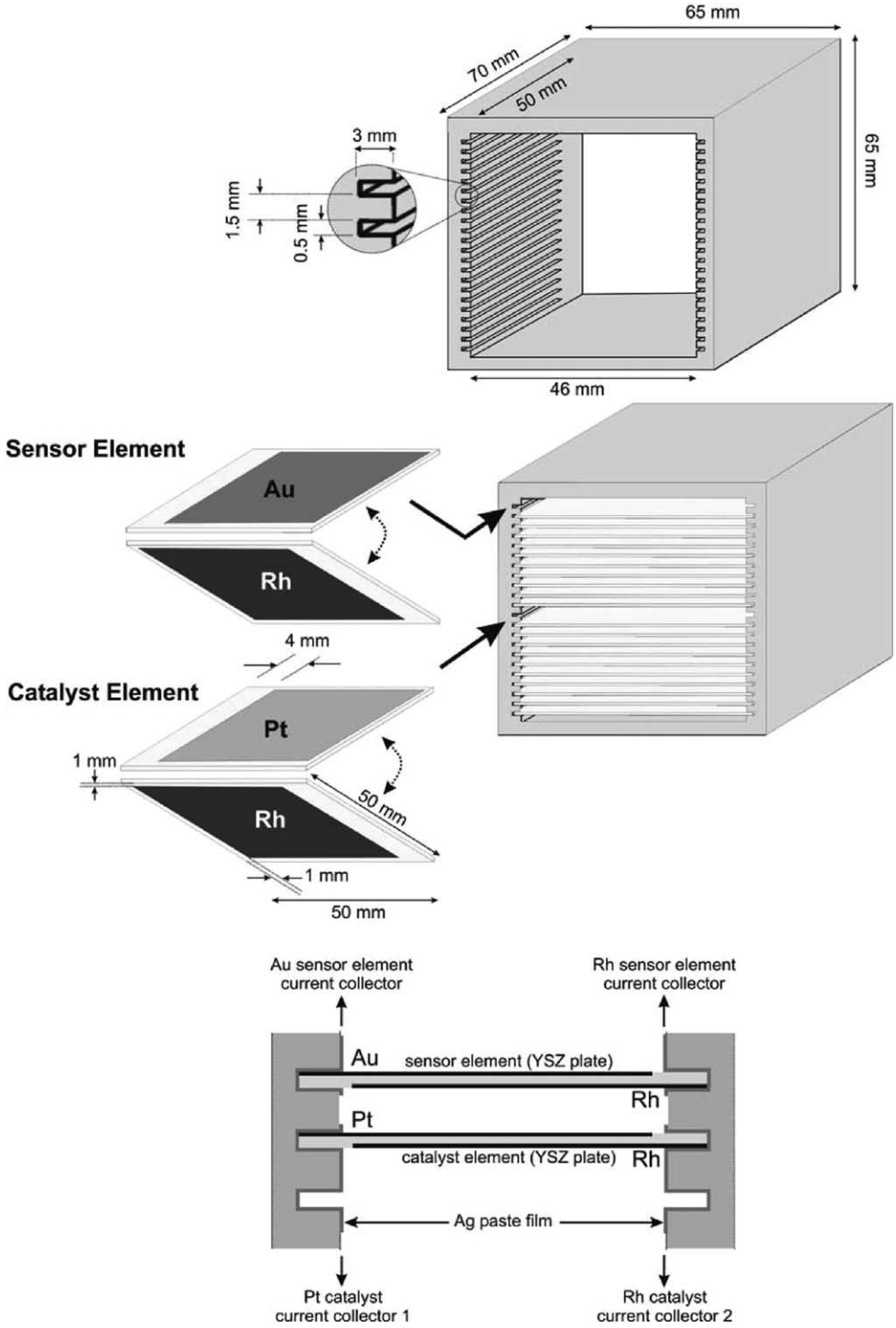

Fig. 7. Schematic and dimensions of the monolithic electropromoted reactor (MEPR) tested with 21 flat Rh/YSZ/Pt plates and one flat Rh/YSZ/Au plate [47]. The bottom figure shows the geometry of the electrical connections on the MEP reactor ceramic walls.

Also it is possible to use one of the plates as a gas-sensor element and utilize the potential signal generated by this element, under open-circuit or at a fixed applied current, to control the current or potential applied to the electropromoted catalytic plates (Fig. 7).

In the first experimental investigation of a MEP reactor [47], the following two reactions were studied:

1. The oxidation of ethylene to CO_2 and H_2O which exhibits strong electrophobic NEMCA behaviour both on Rh [14,52] and on Pt [1,14].
2. The reduction of NO_x by ethylene in presence of O_2, a reaction which is electropromoted predominantly by positive current on Rh [30,52,53] (electrophobic behaviour) and predominantly by negative current on Pt

[14,52,54] (electrophilic behaviour). This dictated the choice of Rh and Pt as catalysts 1 and 2 respectively in the MEP reactor (Fig. 7, [47]). In this way one obtains a synergistic effect of the electropromotion of Rh and Pt deposited on Y_2O_3-stabilized-ZrO_2 (YSZ), when the Rh film is made positive and the Pt film negative. Of course, with this choice of metals one does not expect a synergistic electropromotion effect in the case of C_2H_4 oxidation, since the reaction is electrophobic on both metals.

The solid electrolyte plates were provided by Bosch [47] had a thickness of 0.25 mm and dimensions of 50 mm × 50 mm. They were made of yttria stabilised zirconia (YSZ, 8 wt.-% Y_2O_3 with a resulting molar composition $Zr_{0.913}Y_{0.087}O_{1.957}$). The starting material had a mean particle size of 0.5 μm. The density in the sintered state was between 5.7 and 5.9 g/cm^3.

The Rh/YSZ/Pt and Rh/YSZ/Au samples were prepared by metal sputtering [47]. Prior to Rh, Pt or Au deposition, no surface treatment was performed. The YSZ support was introduced into the sputtering chamber, filled with pure argon, then metal (Rh 99.8 or Pt 99.99, Lesker, or Au 99.99, Metalor) was deposited onto the substrate at 50 °C. The sputtering conditions were the following: direct-current (DC) mode with a discharge of 350 V, argon pressure of 0.5 Pa. Under these conditions the deposition rate is 0.10–0.15 nm/s. The film thickness was measured by calibration with smooth silicon samples processed simultaneously. The thickness of the sputter-deposited rhodium, platinum and gold films was 40 nm.

The surface area of the Rh catalyst films, as well as the metal dispersion was estimated using the galvanostatic transient technique [13,14], by measuring the time constant, τ, required for the rate increase, Δr, in galvanostatic electropromotion rate transients to reach 63% of its steady state value. In this way one can estimate the reactive oxygen uptake, N_G, of the Rh film and, assuming a 1:1 surface Rh:O ratio, the active catalyst surface area, N_G, expressed in mol, from [13,14]:

$$\tau = \frac{2FN_G}{I} \quad (3)$$

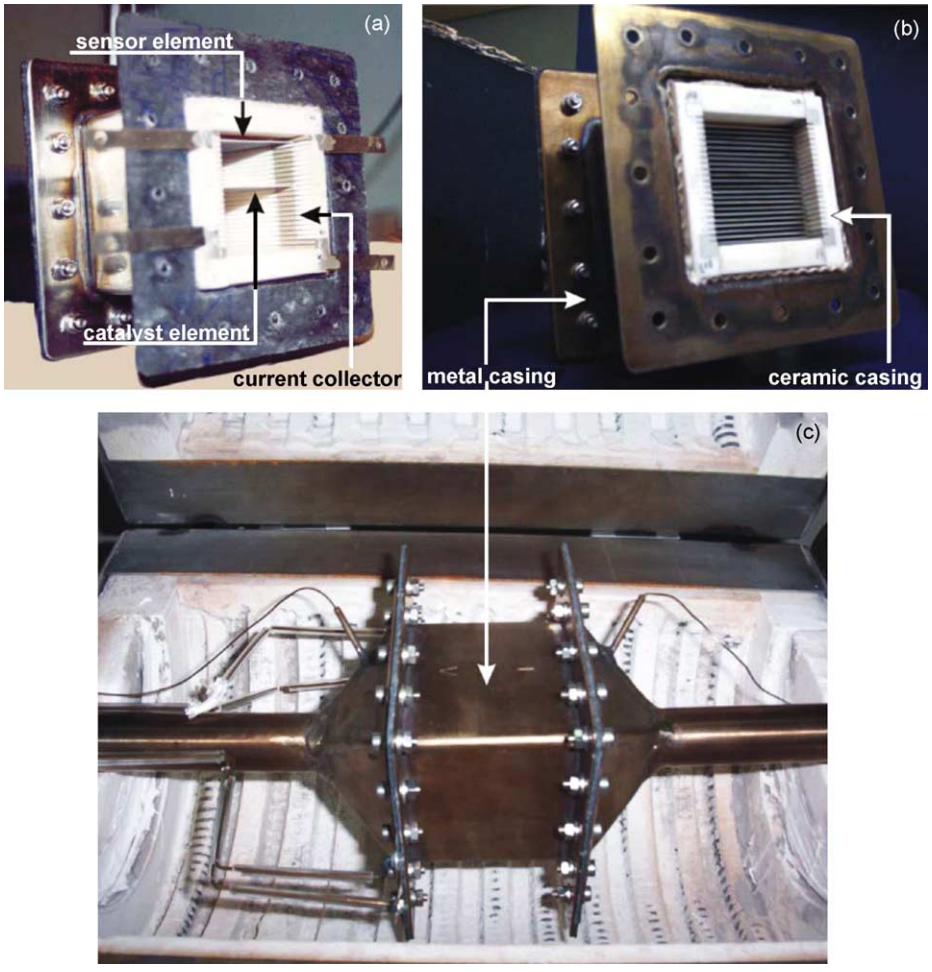

Fig. 8. Photographs of the MEP reactor-sensor showing: (a) the machinable ceramic reactor walls, one of the Ag current collectors on the wall, the plate location for two-plate operation (top plate was used as sensor element) and part of the metal casing; (b) the 22 plate unit (c) the assembled reactor with metal casing in the furnace. Also shown are the two thermocouple housings and the four shielded electrical connections for sensing and electropromotion [47].

This estimation of the Rh catalyst surface area, based on galvanostatic transients during C_2H_4 oxidation, is possible due to the fact that, as discussed in [47], the overall rate of C_2H_4 oxidation exhibits overall electrophobic behaviour over the Rh/YSZ/Pt catalyst plates, i.e., is enhanced with positive applied current and potential, i.e. with O^{2-} supply to the Rh catalyst film. The thus estimated metal Rh dispersion is 13–40% [47], i.e. comparable to that of commercial supported catalysts.

In the first MEPR study [47], we have presented results obtained with a MEP reactor using 1 or 22 Pt/YSZ/Rh plates, where the thin (40 nm) Pt and Rh films were deposited on the opposing sides of the thin (0.25 mm) YSZ plates.

Here we show results obtained in the same reactor (Fig. 8) with ten similar Rh/YSZ/Au plates for the case of C_2H_4 oxidation (Fig. 9) and NO reduction by C_2H_4 in presence of O_2 (Fig. 10). The Rh thin films were sputtered as described above, while paste Au electrodes [14] were used as counterelectrodes. As shown in these figures both the MEP reactor and the thin (40 nm) sputtered Rh catalyst films operate very well and exhibit non-Faradaic performance even at quite high reactant conversions. The same MEP reactor has been recently operated successfully at total gas flowrates of 25 l/min. This corresponds to a space velocity of 12,000 h^{-1}, which is in the same order of magnitude as practical exhaust treatment units. It is important to emphasize that this has been accomplished, with similar noble metal dispersion (10–30%) as in state-of-the-art exhaust treatment catalysts.

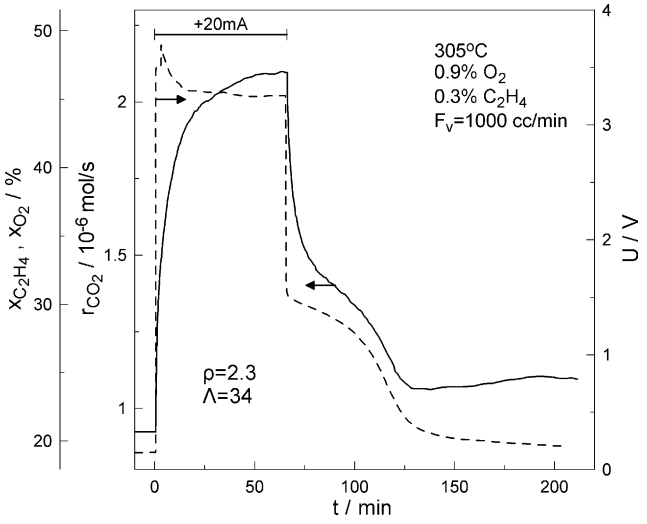

Fig. 9. Ten-plate MEPR operation with C_2H_4 oxidation on Rh: transient response of the rate of CO_2 formation and of the conversions of O_2 and C_2H_4 upon application of a constant anodic current in the MEP reactor loaded with 10 catalyst plates (Rh/YSZ/Au) and one sensor element; $T = 305$ °C.

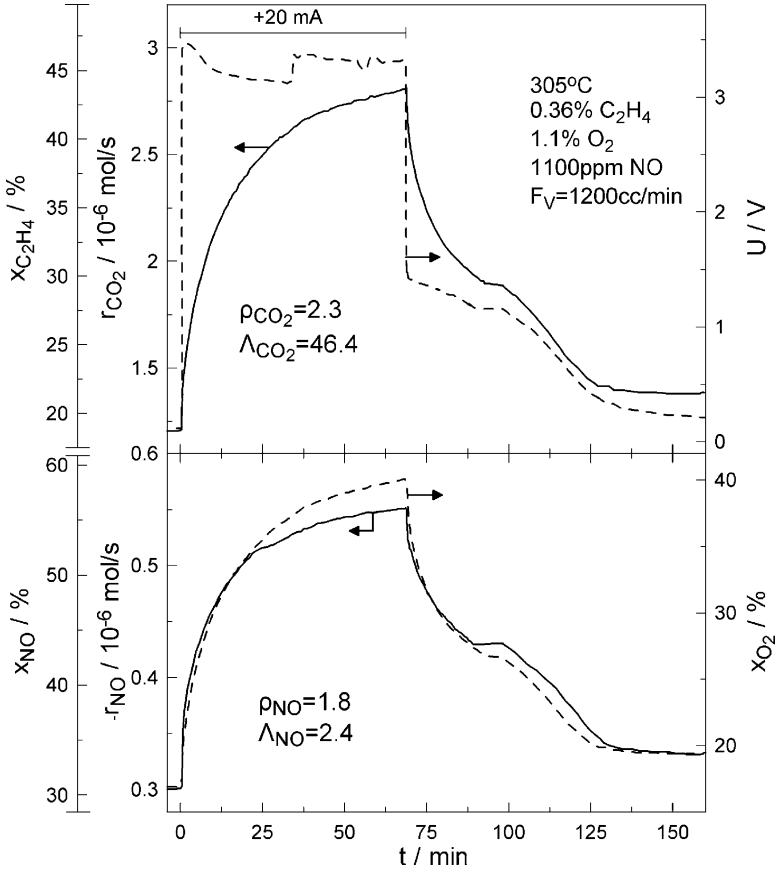

Fig. 10. Ten-plate MEPR operation with NO reduction by C_2H_4 in presence of O_2: transient effect of constant applied anodic current (+20 mA) on the catalytic rates of CO_2 production (r_{CO_2}) and NO reduction ($-r_{NO}$), on the NO conversion (x_{NO}) and on the Rh-Au potential difference (U), $T = 305$ °C.

4. Outlook

The recent advances in electropromoted reactor design and operation ([47] and Figs. 7–10) have shown that electrochemical promotion may soon find practical applications in exhaust treatment units and in chemical destruction or synthesis processes. Several aspects related to durability, useful lifetime, electrolyte and stack cost minimization, scale-up and scale-down have not yet been addressed in any detail, but there is already strong industrial interest and involvement (e.g. [47]) and the next 5 years are likely to lead to commercialization of some electropromoted reactors.

Acknowledgments

We thank the PENED programme of the HSRT and the Growth programme of the EU for financial support.

References

[1] C.G. Vayenas, S. Bebelis, S. Ladas, Nature 343 (1990) 625.
[2] J. Pritchard, Nature 343 (1990) 592.
[3] R.M. Lambert, F. Williams, A. Palermo, M.S. Tikhov, Topics Catal. 13 (2000) 91.
[4] G. Foti, S. Wodiunig, C. Comninellis, Curr. Topics Electrochem. 7 (2001) 1.
[5] C.A. Cavalca, G.L. Haller, J. Catal. 177 (1998) 389.
[6] L. Ploense, M. Salazar, B. Gurau, E.S. Smotkin, JACS 119 (1997) 11550.
[7] P. Vernoux, F. Gaillard, L. Bultel, E. Siebert, M. Primet, J. Catal. 208 (2002) 412.
[8] I. Metcalfe, J. Catal. 199 (2001) 247;
I. Metcalfe, J. Catal. 199 (2001) 259.
[9] C. Sanchez, E. Leiva, in: W. Vielstich, H. Gasteiger, A. Lamm (Eds.), Handbook of Fuel Cells: Fundamentals, Technology and Applications, vol. 2, Wiley, England, 2003.
[10] G.-Q. Lu, A. Wieckowski, Curr. Opin. Colloid Interf. Sci. 5 (2000) 95.
[11] B. Grzybowska-Swierkosz, J. Haber, Annual reports on the Progress of Chemistry, The Royal Society of Chemistry, Cambridge, 1994.
[12] J.O.M. Bockris, Z.S. Minevski, Electrochim. Acta 39 (1994) 1471.
[13] C.G. Vayenas, M.M. Jaksic, S. Bebelis, S.G. Neophytides, in: J.O.M. Bockris, B.E. Conway, R.E. White (Eds.), Modern Aspects of Electrochemistry, vol. 29, Kluwer Academic/Plenum Publishers, New York, 1996, p. 57.
[14] C.G. Vayenas, S. Bebelis, C. Pliangos, S. Brosda, D. Tsiplakides, Electrochemical Activation of Catalysis: Promotion, Electrochemical Promotion and Metal–Support Interactions, Kluwer Academic/Plenum Publishers, New York, 2001, references therein.
[15] A. Wieckowski, E. Savinova, C.G. Vayenas (Eds.), Catalysis and Electrocatalysis at Nanoparticles, Marcel Dekker Inc., New York, 2003.
[16] L.L. Hegedus, R. Aris, A.T. Bell, M. Boudart, N.Y. Chen, B.C. Gates, W.O. Haag, G.A. Somorjai, J. Wei, Catalyst Design: Progress and Perspectives, Wiley, New York, 1987.
[17] M.C.J. Bradford, M.A. Vannice, Catal. Today 50 (1999) 87.
[18] S.J. Tauster, S.C. Fung, R.L. Garten, JACS 100 (1978) 170.
[19] G.L. Haller, D.E. Resasco, Adv. Catal. 36 (1989) 173.
[20] E.C. Akubuiro, X.E. Verykios, J. Catal. 103 (1987) 173;
E.C. Akubuiro, X.E. Verykios, J. Catal. 113 (1988) 106.
[21] X.E. Verykios, in: A. Wieckowski, E.R. Savinova, C.G. Vayenas (Eds.), Catalysis and Electrocatalysis at Nanoparticles Surfaces, Marcel Dekker Inc., New York, 2003, p. 745.
[22] M. Haruta, A. Ueda, S. Tsubota, R.M.T. Sanchez, Catal. Today 29 (1996) 443.
[23] B.L. Mojet, J.T. Miller, D.E. Ramaker, D.C. Konigsberger, J. Catal. 186 (1999) 373.
[24] R.J. Farrauto, C.H. Bartholomew, Fundamentals of Industrial Catalytic Processes, Chapman and Hall, London, 1997.
[25] S. Kuba, P. Lukinskas, R.K. Grasselli, B.C. Gates, H. Knoezinger, J. Catal. 216 (2003) 353.
[26] J. Nicole, D. Tsiplakides, C. Pliangos, X.E. Verykios, C. Comninellis, C.G. Vayenas, J. Catal. 204 (2001) 23.
[27] C. Vayenas, D. Archonta, D. Tsiplakides, J. Electroanal. Chem. 554-555 (2003) 301.
[28] C. Pliangos, I.V. Yentekakis, V.G. Papadakis, C.G. Vayenas, X.E. Verykios, Appl. Catal. B 14 (1997) 161.
[29] C.G. Vayenas, G. Pitselis, I&EC Res. 40 (2001) 4209.
[30] C.G. Vayenas, S. Brosda, C. Pliangos, J. Catal. 216 (2003) 487.
[31] C.G. Vayenas, S. Bebelis, I.V. Yentekakis, H.-G. Lintz, Catal. Today 11 (3) (1992) 303.
[32] C.G. Vayenas, I.V. Yentekakis, S.I. Bebelis, S.G. Neophytides, Ber. Buns. Phys. Chem. 99 (11) (1995) 1393.
[33] C.G. Vayenas, S. Neophytides, Electrochemical activation of catalysis: in situ controlled promotion of catalyst surfaces, Catalysis-Special periodical report, Royal Society of Chemistry, Cambridge, 1996, pp. 199–253.
[34] C.G. Vayenas, S. Bebelis, I.V. Yentekakis, S. Neophytides, Electrocatalysis and electrochemical reactors, in: P.J. Gellings, H.J.M. Bouwmeester (Eds.), CRC Handbook on Solid State Ionics, CRC Press Inc., Boca Raton, 1997, , pp. 445–480.
[35] C.G. Vayenas, I.V. Yentekakis, Electrochemical modification of catalytic activity, in: G. Ertl, H. Knötzinger, J. Weitcamp (Eds.), Handbook of Catalysis, VCH Publishers, Weinheim, 1997, , pp. 1310–1338.
[36] G. Fóti, I. Bolzonella, Ch. Comninellis, in: C.G. Vayenas, B.E. Conway, R.E. White (Eds.), Modern Aspects of Electrochemistry—Electrochemical Promotion of Catalysis, vol. 36, Kluwer Academic/Plenum Publishers, New York, 2003.
[37] R. Lambert, in: A. Wieckowski, E.R. Savinova, C.G. Vayenas (Eds.), Catalysis and Electrocatalysis at Nanoparticles Surfaces, Marcel Dekker Inc., New York, 2003, , p. 583.
[38] C. Koutsodontis, A. Katsaounis, C.G. Vayenas, J. Catal., 2004, submitted for publication.
[39] N. Kotsionopoulos, S. Bebelis, Proceedings of the 55th Annual Meeting of the ISE, Thessaloniki, Greece, 2004, p. 1373; J. Appl. Electrochem., 2004, submitted for publication.
[40] M. Ouzounidou, A.D. Skodra, Ch.K. Kokkofitis, M. Stoukides, M. Ishii, Proceedings of the 8th Panhellenic Symposium on Catalysis, Cyprus, 2004, p. 241.
[41] D. Tsiplakides, S. Neophytides, O. Enea, M.M. Jaksic, C.G. Vayenas, J. Electrochem. Soc. 144 (6) (1997) 2072.
[42] E. Lamy-Pitara, S.E. Mouahid, J. Barbier, Electrochim. Acta 45 (2000) 4299.
[43] S. Neophytides, D. Tsiplakides, P. Stonehart, M. Jaksic, C.G. Vayenas, Nature 370 (1994) 292.
[44] I.M. Petrushina, V.A. Bandur, F. Cappeln, N.J. Bjerrum, J. Electrochem. Soc. 147 (8) (2000) 3010.
[45] C. Pliangos, I.V. Yentekakis, S. Ladas, C.G. Vayenas, J. Catal. 159 (1996) 189.
[46] P. Petrolekas, S. Balomenou, C.G. Vayenas, J. Electrochem. Soc. 145 (4) (1998) 1202.
[47] S. Balomenou, D. Tsiplakides, A. Katsaounis, S. Thiemann-Handler, B. Cramer, G. Foti, Ch. Comninellis, C.G. Vayenas, Appl. Catal. B 52 (2004) 181.
[48] S. Brosda, C.G. Vayenas, J. Wei, J. Catal., 2004, submitted for publication.

[49] A. Katsaounis, Z. Nikopoulou, X.E. Verykios, C.G. Vayenas, J. Catal. 222 (2004) 192.
[50] E.A. Baranova, A. Thursfield, S. Brosda, G. Fóti, Ch. Comninellis, C.G. Vayenas, J. Electrochem. Soc. 152 (2) (2005), in press.
[51] J.N. Michaels, C.G. Vayenas, L.L. Hegedus, J. Electrochem. Soc. 133 (3) (1986) 522.
[52] C. Pliangos, I.V. Yentekakis, X.E. Verykios, C.G. Vayenas, J. Catal. 154 (1995) 124.
[53] C. Pliangos, C. Raptis, T. Badas, C.G. Vayenas, Solid State Ionics 136–137 (2000) 767.
[54] M. Marwood, A. Kaloyannis, C.G. Vayenas, Ionics 2 (1996) 302.